THE JOURNAL OF PHYSICAL CHEMISTRY B LETTERS

2005, *109,* 1648−1651
Published on Web 01/15/2005

Crystal-Face Dependences of Surface Band Edges and Hole Reactivity, Revealed by Preparation of Essentially Atomically Smooth and Stable (110) and (100) n-TiO_2 (Rutile) Surfaces

Ryuhei Nakamura,[†] Naomichi Ohashi,[†] Akihito Imanishi,[†] Takeo Osawa,[‡] Yuji Matsumoto,[‡] Hideomi Koinuma,[‡,§] and Yoshihiro Nakato*[,†,§]

Division of Chemistry, Graduate School of Engineering Science, Osaka University, Toyonaka, Osaka 560-8531, Japan, Materials and Structures Laboratory, Tokyo Institute of Technology, Nagastuta Midori-ku, Yokohama 226-8503, Japan, and CREST, JST

Received: November 19, 2004; In Final Form: December 26, 2004

Essentially atomically smooth (100) and (110) n-TiO_2 (rutile) surfaces were prepared by immersion of commercially available single-crystal wafers in 20% HF, followed by annealing at 600 °C in air. The obtained surfaces were stable in aqueous solutions of pH 1−13, showing no change in the surface morphology on an atomic level, contrary to atomically flat surfaces prepared by ion sputtering and annealing under UHV. The success in preparation of the atomically smooth and stable n-TiO_2 surfaces enabled us to reveal clear crystal-face dependences of the surface band edges and hole reactivity in aqueous solutions.

Introduction

Titanium dioxide (TiO_2) and related metal oxides have attracted keen attention recently in view of solar-to-chemical conversion (water splitting)[1] and photocatalytic environmental cleaning.[2] Strong merits of these materials lie in the high photooxidation ability and the chemical stability. A serious shortcoming of large band gaps for these materials is now about to be overcome by findings[3] that doping with N, S, C, or other elements leads to extension of the photoactive region to the visible light. For realizing practicable efficient systems, the understanding of photoreaction mechanisms at atomically well-defined surfaces is of crucial importance.

To date, the atomically well-defined TiO_2 surfaces have been prepared by a method of Ar^+-ion sputtering and thermal annealing under ultrahigh vacuum (UHV) conditions.[4a] Very recently, some studies were reported by using this method on the influence of atomic arrangements of the (110), (100), and (001) TiO_2 (rutile) surfaces on catalytic[4a,d] and photocatalytic[4b,c,e−g] reactions of adsorbed molecules. However, we have to note that the TiO_2 surfaces prepared under UHV are quite different in structures and properties from those in actual photocatalyst systems, in which the TiO_2 surfaces are in contact with aqueous solutions or air. For the TiO_2 surfaces in contact with aqueous solutions, significant reconstruction, including hydrolysis and ion adsorption, should occur. The same holds for the surfaces placed in air because it is reported[5] that more than several monolayers of water are adsorbed on them at room temperature.

There is another problem in the atomically flat surfaces prepared by the Ar^+-ion sputtering and thermal annealing under UHV. Onishi et al. reported[6] that the atomically flat TiO_2 (rutile) (110) surfaces prepared by this method became morphologically rough after exposition to neutral or alkaline aqueous solutions. This implies that the surfaces of this type are unstable in aqueous solutions.

In the present paper, we report that essentially atomically smooth TiO_2 (rutile) (110) and (100) surfaces are prepared by an alternative method of chemical etching and thermal annealing under the atmosphere.[7] Interestingly, the TiO_2 surfaces prepared by this method were stable in aqueous solutions of pH 1−13, suggesting that they were free from damage and defects that may induce etching reactions. The investigations of crystal-face dependences of surface band edges and hole reactivity became possible by this success in preparation of such atomically smooth and stable TiO_2 surfaces.

Experimental Section

Single-crystal rutile n-TiO_2 (99.99% in purity) wafers, doped with 0.05 wt % Nb oxide, were obtained from Earth Chemical Co., Ltd. The wafers were of an n-type as they were, because a very small amount of doped Nb^{4+} acted as an electron donor. The surfaces of the wafers were cut in parallel to the (100) and (110) faces and polished mechanochemically with an alkaline solution of colloidal silica particles. The atomically smooth surfaces were obtained by a procedure of washing with acetone, immersing in 20% HF for 10 min, washing with water, drying in a nitrogen stream, and annealing at 600 °C for 1 h in air. X-ray photoelectron spectroscopic (XPS) analysis showed that no fluorine atom was left at the surface.

Surface morphology was inspected with an atomic force microscope (AFM, Digital Instruments NanoScope IIIa) at room temperature, the samples being placed in air. All AFM images were obtained in a tapping mode with a silicon tip (Digital Instruments) at a driving frequency of about 280 kHz and a scan rate of 1.5 Hz. Low energy electron diffraction (LEED)

* Corresponding author. E-mail: nakato@chem.es.osaka-u.ac.jp.
[†] Osaka University.
[‡] Tokyo Institute of Technology.
[§] CREST, JST.

10.1021/jp044710t CCC: $30.25

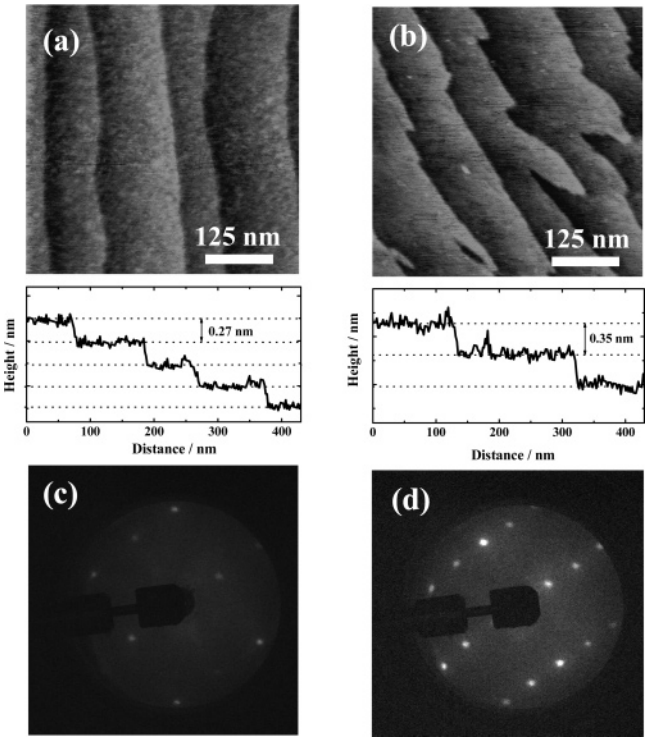

Figure 1. (a) and (b) AFM images and (c) and (d) LEED patterns, for the (100)- and (110)-cut surfaces, respectively, of 0.05 wt % Nb-doped TiO_2 (rutile) single-crystal wafers after surface-smoothing treatments of immersion in 20% HF for 10 min and annealing at 600 °C for 1 h in air.

measurements were carried out with the electron energy of 103 eV under a vacuum of 1×10^{-10} Torr at room temperature. In both the AFM and LEED experiments, the as-prepared surfaces were used as samples with no additional pretreatment.

Photocurrent density (j) vs potential (U) curves for single-crystal n-TiO_2 electrodes were measured with a commercial potentiostat and a potential programmer, using a Pt plate as the counter electrode and an Ag/AgCl/sat. KCl electrode as the reference electrode. The illumination was carried out by the 365 nm band from a 500 W high-pressure mercury lamp, obtained by use of band-pass filters. The PL intensity (I_{PL}) vs U curves were measured simultaneously with the $j-U$ curve measurements. Electrolyte solutions were prepared by use of regent-grade chemicals and pure water, the latter of which was obtained from deionized water by purification with a Milli-Q Water Purification System. The electrolyte solutions under experiments were bubbled with a nitrogen gas to remove dissolved O_2.

Results and Discussion

The surfaces of the commercially obtained n-TiO_2 wafers were not smooth on an atomic scale, with a number of depressions and grooves of 0.2−0.8 nm in depth, as reported previously,[8] suggesting that a variety of crystal faces were exposed. Actually, the wafers showed no distinct difference in the surface band edges and the photoelectrochemical behavior between the (110)- and (100)-cut surfaces. However, the aforementioned procedure of immersion in 20% HF and annealing at 600 °C largely changed the surface morphology. Parts a and b of Figure 1 show AFM images for the (100)- and (110)-cut surfaces after the above procedure. Both the surfaces showed clear step and terrace structures, with the step height of 0.27 nm for the (100) surface and 0.35 nm for the (110) surface, which are in good agreement with the corresponding

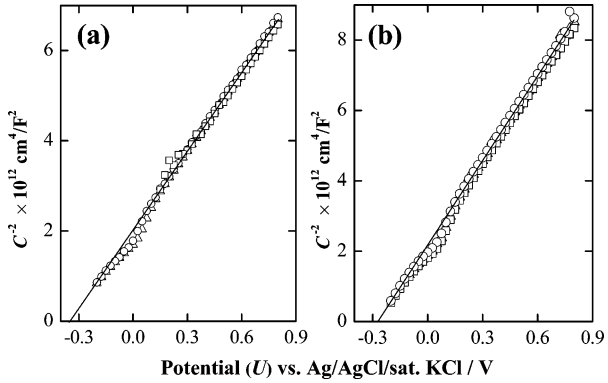

Figure 2. (a) and (b) Mott−Schottky plots for the atomically flat (100) and (110) TiO_2 (rutile) surfaces, respectively: (○) 10 Hz; (△) 100 Hz; (□) 1000 Hz. Electrolyte: 0.1 M $HClO_4$.

step heights in a crystal model of rutile TiO_2 [0.25 nm for (100) and 0.36 nm for (110)]. One may note that some protrusions with the height lower than the single-step height exist in the terrace part of the AFM topography in Figure 1a,b. This will probably be due to experimental noises, though we cannot exclude completely a possibility that small atomic clusters exist here and there at the terrace. We can thus conclude that essentially atomically smooth surfaces are prepared by the present method.

Parts c and d of Figure 1 show LEED patterns for the same (100) and (110) surfaces as above. Both the surfaces gave sharp intense (1 × 1) LEED spots, indicating the formation of essentially atomically smooth (100) and (110) surfaces, in agreement with the AFM experiments. We have to note here that no change in the surface morphology occurred by exposition to aqueous solutions of pH 1−13, i.e., 0.1 M $HClO_4$, 0.05 M Na_2SO_4 (pH 6.5), pure water, and 0.1 M NaOH, for 90 min, indicating that the atomically smooth (100) and (110) surfaces prepared by the present method were stable enough in aqueous solutions, contrary to the surfaces prepared by the ion sputtering and annealing under UHV.[6]

We next investigated the crystal-face dependences of the surface band edges and water photooxidation reaction by using the TiO_2 wafers with the atomically smooth and stable (100) and (110) surfaces. The n-TiO_2 electrodes were prepared by obtaining ohmic contact with indium−gallium alloy. The surface band edge, or the bottom of the conduction band at the surface of n-TiO_2 (E_c^s) was estimated from the flat-band potential (U_{fb}) by the following equation, which holds if the E_c^s and U_{fb} are measured with respect to the same reference level,

$$E_c^{\,s} = -qU_{fb} + \Delta \qquad (1)$$

where q is the elementary charge and Δ is a small energy difference between the bottom of the conduction band (E_c) and the Fermi level (E_F) in the interior of a semiconductor. The U_{fb} was determined from Mott−Schottky plots, i.e., plots of the inverse square of the differential capacitance (C) of the n-TiO_2 electrode against the applied electrode potential (U). The C was measured with a Solartron 1260 impedance analyzer combined with a Solartron 1287 potentiostat at the modulation frequency (f) of 10 to 1000 Hz and the amplitude of 5 mV.

Parts a and b of Figure 2 show the Mott−Schottky plots for n-TiO_2 electrodes with the atomically smooth (100) and (110) surfaces, respectively. Good straight lines were obtained with no deviation by change in the modulation frequency, indicating that the electrode surfaces were really free from damage and

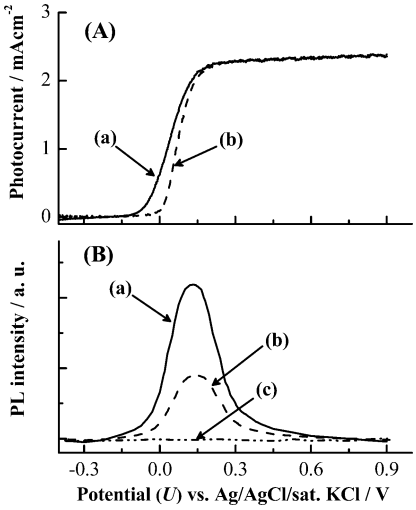

Figure 3. (A) Photocurrent density vs potential (*U*) and (B) the PL intensity vs *U* for the TiO_2 (rutile) surfaces: (a) atomically flat (100) surface; (b) atomically flat (110) surface; (c) commercially obtained (110)-cut surface with no surface-smoothing treatment. Electrolyte: 0.1 M $HClO_4$.

defects. In fact, such frequency-independent good straight lines for n-TiO_2 were first obtained in the present work. The flat-band potential (U_{fb}) was determined from intersection of extrapolation of the straight line with the *U* axis. Interestingly, the U_{fb} for the (100) surface in 0.1 M $HClO_4$ (pH 1.0), determined to be -0.34 ± 0.01 V, was about 0.10 V more negative than that for the (110) surface, -0.25 ± 0.01 V. A similar difference in the U_{fb} was obtained in 0.1 M NaOH (pH 12.7), namely, the U_{fb} for the (100) surface in 0.1 M NaOH was determined to be -1.06 ± 0.01 V, whereas that for the (110) was -0.98 ± 0.01 V. The U_{fb} for both surfaces shifted with pH at a rate of -59 mV/pH. The crystal-face dependence of the U_{fb} was reported for anatase-type TiO_2 in an acidic solution though the surface structure in this case was not regulated on an atomic scale.[9]

The water photooxidation reaction on n-TiO_2 was investigated by measurements of the photocurrent density (*j*) vs *U* and the photoluminescence (PL) intensity (I_{PL}) vs *U*. Figure 3A compares the *j* vs *U* for the atomically smooth (110) and (100) n-TiO_2 electrodes, where the anodic photocurrent is due to oxygen photoevolution (or water photooxidation). The onset potential of the photocurrent for the (100) surface was about 0.1 V more negative than that for the (110) surface, in agreement with the negative shift in the U_{fb} mentioned above. As the onset potential of the photocurrent is deviated from the U_{fb} to the positive for both the (110) and (100) surfaces, the result may indicate that surface carrier recombination is similar between these surfaces. The *j* vs *U* for the commercially obtained (110)- and (100)-cut n-TiO_2 electrodes with no surface-smoothing treatment were rather similar to that for the atomically smooth (110) electrode.

Figure 3B shows the I_{PL} vs *U* for the atomically smooth (110) and (100) n-TiO_2 electrodes, together with the commercially obtained (110)-cut n-TiO_2 with no surface-smoothing treatment for reference. A clear crystal-face dependence of the PL emission was observed, i.e., the PL band, peaked at 840 nm,[10] from the atomically smooth (100) surface was much higher in intensity than that from the atomically smooth (110) surface, and no PL was observed from the commercially obtained (110)-cut [and (100)-cut] surfaces with no surface-smoothing treatment. A similar conclusion was reported in a previous paper;[8,11] namely, we reported[8,11] that the photoetching of n-TiO_2 (rutile) in aqueous H_2SO_4 led to selective exposition of the (100) face and that the PL was observed only for the photoetched [thus the (100)-face exposed] n-TiO_2 electrode. Such sharp crystal-face dependences clearly indicate that the PL band is due to surface carrier recombination, not due to bulk carrier recombination. This assignment is in agreement with the fact that the PL is observed only in a potential region near the onset potential of photocurrent. The disappearance of the PL at potentials much more negative than the onset potential can be attributed[10a,e] to the formation of reduced surface species such as Ti^{3+} at these negative potentials, with which photogenerated holes recombine nonradiatively.

Now, let us consider what is the PL emitting species and why the (100) face shows strong PL emission. We reported in a previous paper[10a,e] that the PL arose from an intermediate (or a precursor) of oxygen photoevolution reaction on n-TiO_2 (rutile). This conclusion was derived from the findings that both the PL and the oxygen photoevolution were suppressed by addition of a suitable reductant to the electrolyte and that a reductant, which suppressed the PL strongly, suppressed the oxygen photoevolution strongly. There was a good correlation between the extent of suppression of the PL and that of the oxygen photoevolution among various reductants. If we consider that the PL and the oxygen photoevolution are suppressed by reaction of photogenerated holes with the added reductant, the above result indicates that the luminescent species acts as an intermediate of the oxygen photoevolution reaction.

We further reported later[8] from studies on the photoetching behavior of n-TiO_2 in aqueous H_2SO_4 that a photogenerated hole coming to the surface was trapped there, resulting in a surface trapped hole (STH), and the oxygen photoevolution (water photooxidation) was initiated by a nucleophilic attack of a water molecule (as a Lewis base) to the STH (as a Lewis acid),

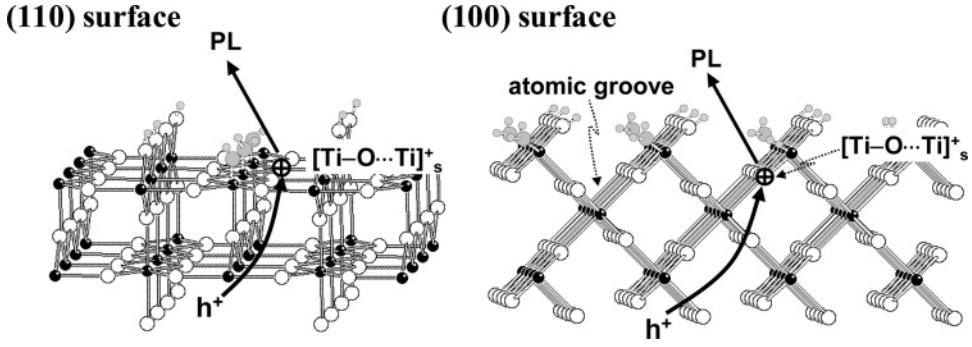

Figure 4. Schematic crystal models for the (110) and (100) TiO_2 (rutile) surfaces in an aqueous electrolyte after consideration of surface reconstruction.

$$[\mathrm{Ti{-}O{-}Ti}]_s + h^+_{VB} \rightarrow [\mathrm{Ti{-}O\cdots Ti}]^+_s \text{ (STH)} \quad (2)$$

$$[\mathrm{Ti{-}O\cdots Ti}]^+_s + H_2O \rightarrow [\mathrm{Ti{-}O^{\bullet}HO{-}Ti}]_s + H^+ \quad (3)$$

where h^+_{VB} refers to a (photogenerated) valence-band hole. This mechanism was recently confirmed by in situ detection of primary surface intermediates of the oxygen photoevolution reaction by multiple internal reflection FTIR spectroscopy[12] and also by studies on the oxygen photoevolution mechanism on visible-light responsive N-doped TiO_2.[13] In these studies, the PL band was assigned,[8,12,13] as a most plausible assignment, to radiative recombination between a conduction-band electron (e^-_{CB}) and a surface-trapped hole, $[\mathrm{Ti{-}O\cdots Ti}]^+_s$.

$$[\mathrm{Ti{-}O\cdots Ti}]^+_s + e^-_{CB} \rightarrow h\nu \text{ (PL)} \quad (4)$$

The strong PL emission from the (100) face can be explained by the above model. The surface-trapped hole (STH) at the (100) face exists at the bottom of atomic grooves, as schematically shown in Figure 4 by a crystal model, or in other words, the STH exists a little inside the surface, covered with Ti−OH groups. Thus, the STH at this face is hardly attacked by an H_2O molecule and kept stable. Accordingly, the STH at this face can accumulate and cause strong PL emission. On the other hand, the STH at the (110) face is directly exposed to the aqueous electrolyte and thus may be relatively easily attacked by an H_2O molecule. This implies that the PL from the (110) face may become weak. For the commercially obtained (110)- and (100)-cut surfaces with no surface-smoothing treatment, a variety of crystal faces (with high index numbers and thus with high-density step and kink sites) are exposed, as mentioned before, and the STH at such surfaces will easily undergo the nucleophilic attack of H_2O through the step and kink sites, resulting in no PL emission. We can thus conclude that the sharp crystal-face dependence of the PL emission reflects that of the reactivity of valence-band holes with aqueous electrolytes.

In conclusion, we have succeeded in preparing the essentially atomically smooth and stable n-TiO_2 (rutile) (100) and (110) surfaces by the method of HF etching and thermal annealing. The success has enabled us to reveal the clear crystal-face dependences of the surface band edges and hole reactivity. TiO_2 and related metal oxides are key materials for solar energy conversion and photocatalytic environmental cleaning. The present work has thus opened a new way to investigate the photocatalytic reactivity and stability of these materials on an atomic level, which is important to search for new active materials.

Acknowledgment. This work was partly supported by a program of NEDO, Japan.

References and Notes

(1) (a) Fujishima, A.; Honda, K. *Nature* **1972**, *238*, 37. (b) Sato, S.; White, J. M. *Chem. Phys. Lett.* **1980**, *72*, 83. (c) Zou, A.; Ye, J.; Sayama, K.; Arakawa, H. *Nature* **2001**, *414*, 625.

(2) (a) Linsebigler, A.; Lu, G.; Yates, J. T., Jr. *Chem. Rev.* **1995**, *95*, 735. (b) Hoffmann, M. R.; Martin, S. T.; Choi, W.; Bahnemann, D. W. *Chem. Rev.* **1995**, *95*, 69.

(3) (a) Sato, S. *Chem. Phys. Lett.* **1986**, *123*, 126. (b) Asahi, R.; Morikawa, T.; Ohwaki, T.; Aoki, K.; Taga, Y. *Science* **2001**, *293*, 269. (c) Ohno, T.; Mitsui, T.; Matsumura, M. *Chem. Lett.* **2003**, *32*, 364. (d) Ishikawa, A.; Takata, T.; Kondo, J. N.; Hara, M.; Kobayashi, H.; Domen, K. *J. Am. Chem. Soc.* **2002**, *124*, 13547. (e) Irie, H.; Watanabe, Y.; Hashimoto, K. *Chem. Lett.* **2003**, *32*, 772.

(4) (a) Diebold, U. *Surf. Sci. Rep.* **2003**, *48*, 53. (b) Henderson, M. A.; White, J. M.; Uetsuka, H.; Onishi, H. *J. Am. Chem. Soc.* **2003**, *125*, 14974. (c) Mezhenny, S.; Maksymovych, P.; Thompson, T. L.; Diwald, O.; Stahl, D.; Walck, S. D.; Yates, J. T., Jr. *Chem. Phys. Lett.* **2003**, *369*, 152. (d) Henderson, M. A. *Surf. Sci. Rep.* **2002**, *46*, 1. (e) Wilson, J. N.; Idriss, H. *J. Am. Chem. Soc.* **2002**, *124*, 11284. (f) Brinkley, D.; Engel, T. *J. Phys. Chem. B* **2000**, *104*, 9836. (g) Linsebrigler, A.; Lu, G.; Yates, J. T., Jr. *J. Phys. Chem. B* **1996**, *100*, 6631.

(5) (a) Nosaka, A. Y.; Fujiwara, T.; Yagi, H.; Akutsu, H.; Nosaka, Y. *J. Phys. Chem. B.* **2004**, *108*, 9121. (b) Suda, Y.; Morimoto, T. *Langmuir* **1987**, *3*, 786.

(6) Uetsuka, H.; Sasahara, A.; Onishi, H. *Langmuir* **2004**, *20*, 4782.

(7) (a) Kawasaki, M.; Takahashi, K.; Maeda, T.; Tsuchiya, R.; Shinohara, M.; Ishiyama, O.; Yonezawa, T.; Yoshimoto, M.; Koinuma, H. *Science* **1994**, *266*, 1540. (b) Yamamoto, Y.; Matsumoto, Y.; Koinuma, H. *Appl. Surf. Sci.* **2004**, *238*, 189.

(8) Kisumi, T.; Tsujiko, A.; Murakoshi, K.; Nakato, Y. *J. Electroanal. Chem.* **2003**, *545*, 99.

(9) Hengerer, R.; Kavan, L.; Krtil, P.; Grätzel, M. *J. Electrochem. Soc.* **2000**, *147*, 1467.

(10) (a) Nakato, Y.; Tsumura, A.; Tsubomura, H. *J. Phys. Chem.* **1983**, *87*, 2402. (b) Nakato, Y.; Ogawa, H.; Moria, K.; Tsubomura, H. *J. Phys. Chem.* **1986**, *86*, 6210. (c) Poznyak. S. K.; Sviridov. V. V.; Kulak. A. I.; Samtsov. M. P. *J. Electroanal. Chem.* **1992**, *340*, 73. (d) Nakato, Y.; Akanuma, H.; Shimizu, J.-I.; Magari, Y. J. *Electroanal. Chem.* **1995**, *396*, 35. (e) Nakato, Y.; Akanuma, H.; Magari, Y.; Yae, S.; Shimizu, J.-I.; Mori, H. *J. Phys. Chem. B* **1997**, *101*, 4934.

(11) Tsujiko, A.; Kisumi, T.; Magari, Y.; Murakoshi, K.; Nakato, Y. *J. Phys. Chem. B* **2000**, *104*, 4873.

(12) Nakamura, R.; Nakato, Y. *J. Am. Chem. Soc.* **2004**, *126*, 1290.

(13) Nakamura, R.; Tanaka, T.; Nakato, Y. *J. Phys. Chem. B* **2004**, *108*, 10617.